International Journal of Electrical, Electronic and Communication Sciences
ISSN: 2517-9438
Vol:12, No:3, 2018

A Tuning Method for Microwave Filter via Complex Neural Network and Improved Space Mapping

Shengbiao Wu, Weihua Cao, Min Wu, Can Liu

***Abstract*—**This paper presents an intelligent tuning method of microwave filter based on complex neural network and improved space mapping. The tuning process consists of two stages: the initial tuning and the fine tuning. At the beginning of the tuning, the return loss of the filter is transferred to the passband via the error of phase. During the fine tuning, the phase shift caused by the transmission line and the higher order mode is removed by the curve fitting. Then, an Cauchy method based on the admittance parameter (Y-parameter) is used to extract the coupling matrix. The influence of the resonant cavity loss is eliminated during the parameter extraction process. By using processed data pairs (the amount of screw variation and the variation of the coupling matrix), a tuning model is established by the complex neural network. In view of the improved space mapping algorithm, the mapping relationship between the actual model and the ideal model is established, and the amplitude and direction of the tuning is constantly updated. Finally, the tuning experiment of the eight order coaxial cavity filter shows that the proposed method has a good effect in tuning time and tuning precision.

***Keywords*—**Microwave filter, scattering parameter (s-parameter), coupling matrix, intelligent tuning.

I. Introduction

THE development of wireless communication and microwave technology has led to more frequency bands in the limited spectrum range. In order to avoid interference between channels, it is necessary to configure high-performance the microwavefilter devices in all systems. However, the performance of the actual microwave filter is difficult to meet the requirements because of the manufacturing error and the material difference. Therefore, tuning after production becomes an essential link. However, tuning is a laborious and time-consuming task. Looking for intelligent tuning methods is our common expectation.

Although the concept of microwave filter tuning was presented several decades ago, the real application began in the 90s of the last century. The intelligent tuning software for microwave filters was developed by Com Dev company as early as 1995 [1], and it was applied to the actual filter tuning in 2003 [2]. Several years later, the fuzzy logic is applied to the tuning of the microwave filter in [3], but the method is only a qualitative analysis of the filter tuning rules, so the tuning accuracy is not very high. Subsequently, the tuning methods in time domain and the method of tuning based on equivalent circuit are also presented [4]. The key links of these methods are the extraction of the coupling matrix. In order to solve this problem, the method of coupling matrix extraction based on S-parameter is emerging. These methods include: optimization method [5], Cauchy method [6], vector fitting method [7] and Jacobian inverse eigenvalue method. However, these methods are not accurate enough for practical filter applications, or have great limitations. In order to solve the coupling matrix extraction in different environments, the coupling matrix extraction method with the source load of the filter is proposed in [8], this method solves the problem that the unload Q value of the resonant cavity is not consistent in the extraction of the coupled matrix. In the literature [9], a vector fitting method based on Y-parameters is proposed, this method can solve the problem of parameter extraction for lossy filter and high-order filter. But due to the sampling point is much larger than the unknown quantity in the actual filter, the method is difficult to obtain accurate coefficients and it is easy to form the sick matrix. In the [10], the phase loading and unloading Q values were extracted by the optimized method, then the coupling matrix is extracted by the synthesis of Chebyshev filter. With the development of microwave technology, many new tuning techniques began to emerge. The time domain tuning method based on the phase of the reflection characteristic is proposed in the literature [11]. This method can deal with the uncertainty of tuning direction in the traditional time domain tuning method. Curve similarity of the filter tuning method is presented in the literature [12], on the basis of maintaining the original curve shape, the method continuously optimizes the feature points on the curve until the desired performance index is reached. But it is difficult to select the feature points of the curve, so it has some influence on the tuning accuracy. In order to avoid the complexity of the extraction of coupling matrix, a filter tuning method based on neural networks is proposed in the literature [13]. The relationship between the return loss and the adjustment of the screws is established by using the neural network. But the drawback of this method is that the tuning model cannot be updated in real time. In order to quickly find the optimal position of the actual filter screws, the space mapping-based

S. Wu is with the School of Automation, China University of Geoscience and Hubei key Laboratory of Advanced Control and Intelligent Automation for Complex Systems, Wuhan, 430074, China and School of Gongqing, Nanchang University, Jiangxi, 332020, China.

W. Cao is with the School of Automation, China University of Geoscience and Hubei key Laboratory of Advanced Control and Intelligent Automation for Complex Systems, Wuhan, 430074, China (corresponding author, e-mail: weihuacao@cug.edu.cn).

M. Wu is with the School of Automation, China University of Geoscience and Hubei key Laboratory of Advanced Control and Intelligent Automation for Complex Systems, Wuhan, 430074, China.

C. Liu is with the School of Automation, China University of Geoscience and Hubei key Laboratory of Advanced Control and Intelligent Automation for Complex Systems, Wuhan, 430074, China.

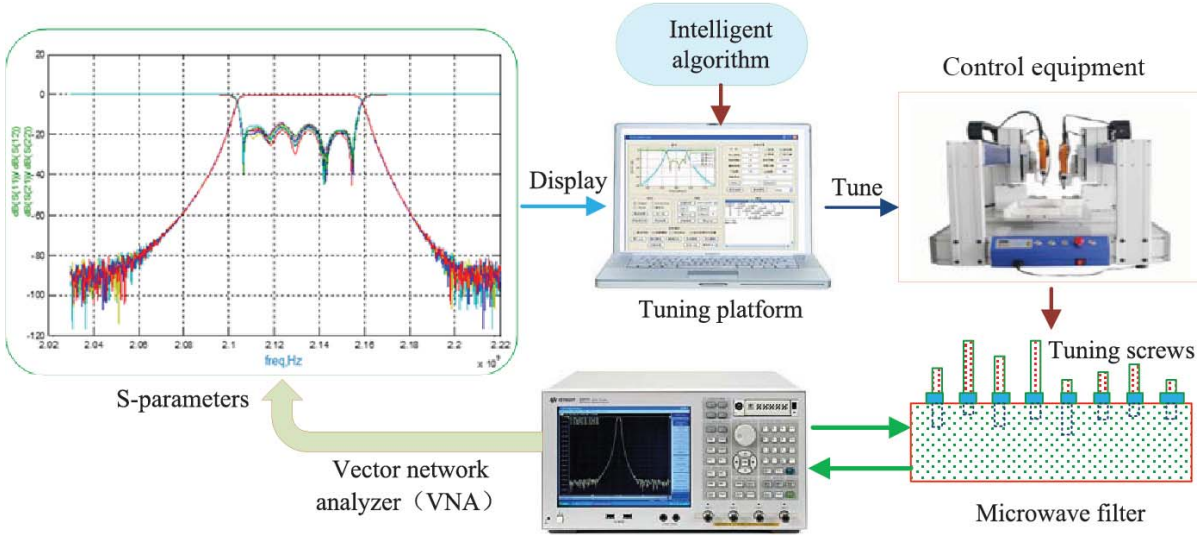

Fig. 1 Intelligent tuning system diagram of microwave filter

tuning method is mentioned in many literatures. Different from the traditional space mapping, the paper [14] makes the response of the rough model close to the fine model by setting the preselected parameters, and constantly optimizes the rough model to reach the ideal target. But when the higher order filter is encountered, the method may be difficult to converge.

The advantage of the method in this paper is that it not only solves the problem of the initial tuning of the filter in the case of large detuning, but also solves the problems of higher power, phase shift and loss in the extraction of parameters. Finally, the hybrid tuning of the microwave filter is performed by using complex neural networks and improved space mapping algorithm. The rest of the paper is arranged as follows: Section 2 introduces the initial tuning of the coaxial cavity filter. The extraction of the coupling matrix is in the Section 3. Section 4 is mainly the modeling and tuning of the coaxial cavity filter. The last part is the conclusion.

II. Initial Tuning of Microwave Filter

The intelligent tuning system of microwave filter mainly consists of four links: The first link is the extraction of the S parameter by vector network analyzer. The second link is the construction of the tuning platform. The third link is the design of intelligent optimization algorithm, and the last link is the control part of the tuning system. Intelligent microwave filter tuning system is shown in Fig. 1.

The key of tuning is to establish the mapping between the ideal model and the actual model, which can guide the iterative optimization direction to find the tuning position of the screws. It is essential for tuning to accurately extract the coupling matrix from the output S-parameters, however, the initial detuning of the filter is very large and it is difficult to extract the coupling matrix from the S-parameters. Therefore, we need to tune the filter by optimizing the zero and pole positions of the reflected parameters. The expressions of the reflection function and phase are as follows:

$$S_{11}(j\omega) = \varepsilon \frac{(s-z_1)(s-z_2)\cdots(s-z_n)}{(s-p_1)(s-p_2)\cdots(s-p_n)}, \tag{1}$$

$$\phi_{s_{11}}(j\omega) = \sum_{poles} \arctan\left(\frac{\omega-\omega_n}{\sigma_n}\right) - \sum_{zeros} \arctan\left(\frac{\omega-\omega_n}{\sigma_n}\right), \tag{2}$$

where ε is the normalized constant of amplitude response, z_n and p_n are the nth zeros and poles of the S_{11} on the coordinate axis (the horizontal axis is σ, and the vertical axis is $j\omega$), and σ_n is the zero pole shift caused by the filter loss. The objective function in the optimization is designed as follows:

$$F = \int_{\omega l}^{\omega h} \left| \phi_{s_{11}}^{i}(j\omega) - \phi_{s_{11}}^{i}{}'(j\omega) \right|^2 d\omega, \tag{3}$$

where $\phi_{s_{11}}^{i}(j\omega)$, $\phi_{s_{11}}^{i}{}'(j\omega)$ represent the phase of the current state and the ideal state, respectively, ωh and ωl are the highest and lowest frequencies of the reflected characteristics.

Fig. 2 shows the comparison of the phase characteristics of the return loss before and after tuning. The results show that

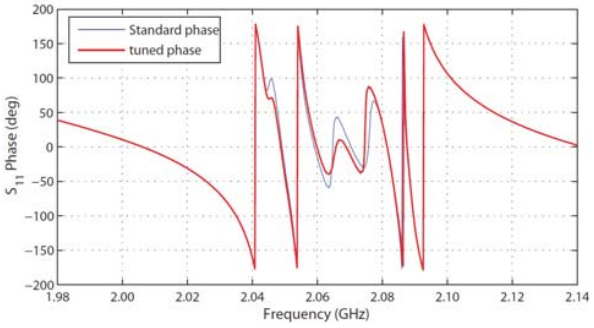

Fig. 2 Comparison of Standard phase and tuned phase

the phase after tuning is highly consistent with the standard phase 180^0. However, not every phase value of the peak can achieve the standard. Therefore, the filter is still required fine tuning.

III. Coupling Matrix Extraction

The output response of the coaxial cavity filter mainly includes the transmission characteristics (S_{12}) and the reflection characteristics (S_{11}). How to extract the parameters closely related to the tuning screw from the output response is important to the tuning. In general, the output response is represented by a coupling matrix, and the extraction process is described below.

A. Elimination of Phase Shift

Generally, the coupling between the resonators of the filter based on the circuit model is realized by the converter, so there is no phase shift phenomenon. However, the filter based on the actual physical model often has phase shift due to the transmission line and the higher order mode. If the phase shift of coaxial filters cannot be effectively eliminated, the accuracy of the admittance parameters decreases, making poles and residues of admittance parameters presenting big deviation, which is unable to realize the extraction of coupling matrix and the S-parameter description. For two-port dissipative network, the scattering parameters of the network are expressed as polynomials:

$$\begin{cases} v_1^- = S_{11}v_1^+ + S_{12}v_2^+ \\ v_2^- = S_{21}v_1^+ + S_{22}v_2^+, \end{cases} \tag{4}$$

where v_1^+ and v_2^+ are incident voltage waves, v_1^- and v_2^- are are reflected voltage waves. After the transmission line is connected, the incident wave and the reflected wave form change as in Fig. 3.

$$v_1^- = e^{j\theta_1} * h_1^- \quad v_2^- = e^{j\theta_2} * h_2^- \tag{5}$$

$$v_1^+ = e^{-j\theta_1} * h_1^+ \quad v_2^+ = e^{-j\theta_2} * h_2^+. \tag{6}$$

At this point, the relation between the scattering matrix of the two port network and the normalized incident (reflected) voltage wave is as follows:

$$\begin{bmatrix} h_1^- \\ h_2^- \end{bmatrix} = \begin{bmatrix} e^{-j\theta_1} & 0 \\ 0 & e^{-j\theta_2} \end{bmatrix} [S] \begin{bmatrix} e^{-j\theta_1} & 0 \\ 0 & e^{-j\theta_2} \end{bmatrix} \begin{bmatrix} h_1^+ \\ h_2^+ \end{bmatrix}. \tag{7}$$

The relationship between the S^{mea} based on the ideal model and the S based on the actual filter model as follows [15]:

$$S_{ij} = \begin{bmatrix} S_{11}^{mea}\exp(-j2\theta_1) & S_{12}^{mea}\exp[-j(\theta_1+\theta_2)] \\ S_{21}^{mea}\exp[-j(\theta_1+\theta_2)] & S_{22}^{mea}(-j2\theta_2) \end{bmatrix}. \tag{8}$$

The phase shift of the actual filter with high order mode and phase loading is as follows [16]:

$$\begin{gathered} \theta_1 = \theta_{01} + \beta\cdot\Delta l \quad \theta_2 = \theta_{02} + \beta\cdot\Delta l \\ \Delta\varphi s_{11} = -2\beta\Delta l \approx -2\Delta l\sqrt{\mu\varepsilon}\omega, \end{gathered} \tag{9}$$

where θ_{01}, θ_{02} are the phase loading, β is the transmission length of the transmission line, and l is the length of the

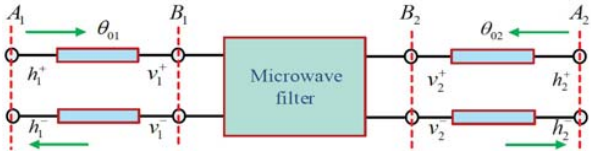

Fig. 3 S-parameter matrix of two port network

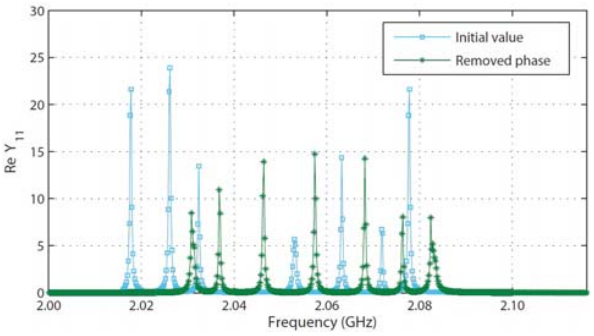

Fig. 4 Comparison of real of Y_{11} before and after phase shift

transmission line. When ω is the normalized frequency, the phase of the reflection characteristic S_{11} is expressed as:

$$\begin{gathered} \varphi_{s_{11}} = \tan^{-1}\frac{b_{n-1}\omega^{n-1} + b_{n-2}\omega^{n-2} + \cdots + b_0}{\omega^n + b_{n-1}\omega^{n-1} + \cdots + b_0} \\ \varphi_{s_{11}} = \frac{k_1}{\omega} \quad \tau_{s_{11}} = \frac{\partial s_{11}}{\partial\omega} \approx -\frac{k_2}{\omega^2} \quad \omega \to \pm\infty, \end{gathered} \tag{10}$$

where k_1 and k_2 are proportional constants, $b_n, b_{n-1}\cdots, b_1$ is the coefficient of the polynomial $E(s)$, The expressions for the phase and group delay of the actual filter are given by combining (9), (10) as follows:

$$\begin{gathered} \varphi_{s_{11}}(\omega) \approx k_1/\omega - 2(\varphi_0 + \beta\cdot\Delta l) \approx k_1/\omega - 2\varphi_0 \\ \tau_{s_{11}} = \frac{\partial s_{11}}{\partial\omega} \approx -\frac{k_2}{\omega^2} - 2\Delta l\sqrt{\mu\varepsilon}. \end{gathered} \tag{11}$$

In the curve fitting, the sampling point which is far from the passband is selected as the object. It can be concluded by experiment that the curve fitting effect is better. The phase shift of I/O port is -74.53^0 and -71.830^0 after fitting. The length of the transmission lines embedded in the ports is 4.4847e-8(m) and 2.8792e-9 (m). In order to facilitate the extraction of the coupling matrix, the S- parameter and the Y-parameter need to be transformed as follows:

$$\begin{gathered} y_{11} = \frac{(1-S_{11})(1+S_{22}) + S_{12}S_{21}}{(1+S_{11})(1+S_{22}) - S_{12}S_{21}} \\ y_{12} = \frac{-2S_{12}}{(1+S_{11})(1+S_{22}) - S_{12}S_{21}}. \end{gathered} \tag{12}$$

In Figs. 4 and 5, the position of the poles and zero of the admittance parameters is improved after phase shift elimination. It improves the unload quality factor of the resonator and the extraction precision of the coupling matrix, which is very helpful for the modeling and tuning of the system.

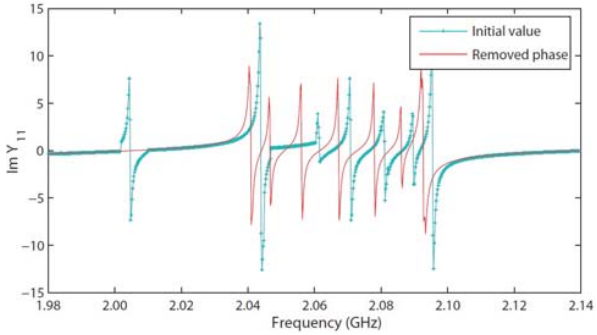

Fig. 5 Comparison of imaginary of Y_{11} before and after phase shift

B. Solution of Coupling Matrix

The existing filter theory is generally based on the lowpass prototype. In order to realize the synthesis of the coaxial cavity bandpass filter, the frequency conversion is essential. $s = j(f_0/Bw)\left(\omega/\omega_0 - \omega_0/\omega\right)$ is used in the bandpass filter. By using the normalized conversion of frequency variable, the synthesis of the low pass filter can be used to deal with the bandpass filter.

The characteristic polynomials of the two-port network admittance parameters are as follow [17]:

$$Y_{11}(s) = \frac{U(s)}{W(s)} = \frac{\sum_{k=0}^{n} a_k^{(1)} s^k}{\sum_{k=0}^{n} b_k s^k} \tag{13}$$

$$Y_{12}(s) = \frac{V(s)}{W(s)} = \frac{\sum_{k=0}^{n} a_k^{(2)} s^k}{\sum_{k=0}^{n} b_k s^k}. \tag{14}$$

where $a^{(1)} = \left[a_n^{(1)}, \cdots, a_0^{(1)}\right]^T$, $a^{(2)} = \left[a_{nz}^{(2)}, \cdots, a_0^{(2)}\right]^T$, $b = [b_n, \cdots, b_1]^T$ are the coefficients of the characteristic polynomial respectively. The formula (13), (14) of the reflection function and the transfer function are transformed as follows:

$$\begin{cases} \sum_{k=0}^{n} a_k^{(1)} s^k - Y_{11}(s_i) \sum_{k=0}^{n} b_k s^k = 0 \\ \sum_{k=0}^{n} a_k^{(2)} s^k - Y_{12}(s_i) \sum_{k=0}^{n} b_k s^k = 0 \end{cases} \tag{15}$$

The starting point of the filter synthesis is to obtain the polynomial coefficient of the S-parameters. In order to improve the precision of the coupled matrix extraction, we need to select the frequency point in the passband when extracting polynomial coefficients. Here, $0_{i\times j} \in R^{i\times j}$ is empty matrix, $Y_{ij} = diag\left\{Y_{ij}(s_k)\right\}_{k=1,2,\cdots N}$, V_n is a Vandermonde matrix with elements $v_{i,k} = (s_i)^{k-1}$, $(k = 1,2,\cdots m+1)$, n is the number of resonators in the filter. N is the number of frequency points. $\sum$ is a diagonal matrix whose elements are the eigenvalues of the M matrix. U and V is a unitary matrix. After all the polynomial coefficients are obtained, The pole and residues of the ideal state can be obtained as shown in Table I.

According to the above $Y_{21}(s)$, $Y_{22}(s)$ of the numerator and denominator polynomial coefficients, it is easy to obtain the admittance matrix expression containing the poles and the remainder by partial fractional expansion [18]:

$$[Y] = j\begin{bmatrix} 0 & K_\infty \\ K_\infty & 0 \end{bmatrix} + \sum_{k=1}^{N} \frac{1}{s - (j\lambda_k - \sigma_k)} \begin{bmatrix} r_{11k} & r_{12k} \\ r_{21k} & r_{22k} \end{bmatrix}. \tag{16}$$

In general, $K_\infty = 0$ except that the transmission zero and order of the filter are equal, λ_k is the eigenvalues of the coupled matrix. $r_{ij}(i = 1,2, j = 1,2)$ is the corresponding residue under its eigenvalue. $\sigma_k = f_0/(Bw \cdot Q_u)$ is a loss factor and Q_u is the unload quality factor, which can be obtained by optimizing algorithms.According to the equivalent circuit of the two port network, the following admittance matrix expression based on the circuit element can be obtained.

$$[Y] = j\begin{bmatrix} 0 & M_{sl} \\ M_{sl} & 0 \end{bmatrix} + \sum_{k=1}^{N} \frac{1}{sC_k + jB_k} \begin{bmatrix} M_{sk}^2 & M_{sk}M_{lk} \\ M_{sk}M_{lk} & M_{lk}^2 \end{bmatrix}, \tag{17}$$

where M_{sk} is the coupling of the source to the kth resonator, M_{lk} is the coupling of the load to the kth resonator, M_{kk} represents the self-coupling of the kth resonator. By comparing the element values of admittance matrix in (16) and (17), the correspondence relationship between coupling matrix elements and the circuit component values is as follows:

$$M_{kk} = -\lambda_k + \sigma_k \quad M_{lk} = \sqrt{r_{22k}} \quad M_{sk} = \sqrt{r_{11k}}. \tag{18}$$

By using the extracted coupling matrix, the curve of the scattering parameters of the filter can be obtained by combining the following formula:

$$\begin{aligned} A &= sI - jR + M' \quad M' = M - j[\sigma_k] \\ S_{11} &= 1 + 2jR_1[A]_{n1}^{-1} \quad S_{21} = -2j\sqrt{R_1 R_n}[A]_{11}^{-1}, \end{aligned} \tag{19}$$

where $[R] = diag[R_1, 0, \cdots 0, R_n]$, $[\sigma_k] = diag[0, \sigma_1, \cdots \sigma_k, 0]$ is the loss of the resonant cavity.

TABLE I
THE RESIDUE AND EIGENVALUE OF COAXIAL CAVITY FILTER

k	r_{21}	r_{22}	λ_k
1	-0.1088+0.0027 j	0.1257+0.0014 j	0.0095-1.2225 j
2	0.1710+0.0033 j	0.1387+0.0043 j	-0.0099-1.1306 j
3	-0.1383+0.0001 j	0.1316+0.0001 j	-0.0094-0.7214 j
4	-0.1508+0.0002 j	0.1435+0.0001 j	-0.0095-0.2368 j
5	-0.1463+0.0001 j	0.1386+0.0014 j	-0.0094-0.2781 j
6	-0.1229+0.0003 j	0.1009+0.0020 j	-0.0090-0.7331 j
7	-0.1114+0.0005 j	0.0529+0.0016 j	-0.0095-1.0923 j
8	-0.0583+0.0005 j	0.2350+0.0063 j	-0.0096-1.2029 j

According to the eigenvalues, poles and residues, combined with the formula (18), the coupling matrix of the filter can be synthesized as shown in Table II.

Since the extracted coupling matrix contains elements that are not needed by the filter, it needs to be further transformed. The converted coupling matrix contains the physical and electrical characteristics of the filter, it can be obtained by rotating transform, as shown in Table III.

The nonzero elements on the diagonal of Table III represent the magnitude of the resonant cavity's deviation from the center frequency, the other nonzero elements represent the coupling between the resonators.

TABLE II
THE INITIAL COUPLING MATRIX OF EXTRACTED

	S	1	2	3	4	5	6	7	8	L
S	0	-0.3068	0.4590	-0.3813	0.3980	-0.3929	0.3870	-0.4577	0.1201	0
1	-0.3068	-0.0342	0	0	0	0	0	0	0	0.3545
2	0.4590	0	0.0142	0	0	0	0	0	0	0.3725
3	-0.3813	0	0	0.0371	0	0	0	0	0	0.3627
4	0.3980	0	0	0	0.1423	0	0	0	0	0.3788
5	-0.3929	0	0	0	0	0.0953	0	0	0	0.3723
6	0.3870	0	0	0	0	0	-0.1975	0	0	0.3176
7	-0.4577	0	0	0	0	0	0	-0.5434	0	0.2433
8	0.1201	0	0	0	0	0	0	0	-0.8824	0.4848
L	0	0.3545	0.3725	0.3627	0.3788	0.3723	0.3176	0.2433	0.4848	0

TABLE III
TRANSFORMED COUPLING MATRIX

	S	1	2	3	4	5	6	7	8	L
S	0	0.1865	0	0	0	0	0	0	0	0
1	0.1865	-0.0342	-0.8337	0	0	0	0	0	0	0
2	0	-0.8337	0.0142	0.6003	0	0	0	0	0	0
3	0	0	0.6003	0.0371	-0.5933	0	0	0	0	0
4	0	0	0	-0.5933	0.1423	-0.6492	0	0	0	0
5	0	0	0	0	-0.6492	0.0953	-0.58	0	0	0
6	0	0	0	0	0	-0.58	-0.1975	0.5542	0	0
7	0	0	0	0	0	0	0.5542	-0.5434	0.5871	0
8	0	0	0	0	0	0	0	0.5871	-0.8824	0.024
L	0	0	0	0	0	0	0	0	0.024	0.0018

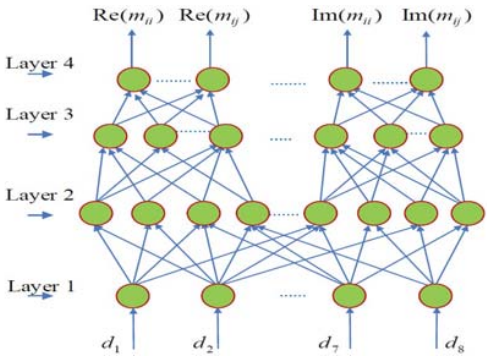

Fig. 6 The Tuning model of coaxial cavity filter

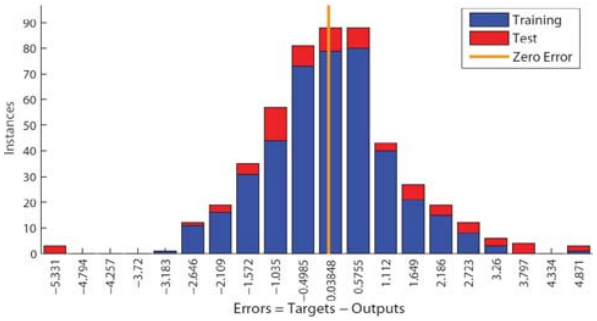

Fig. 7 The Error Histogram of the Tuning model

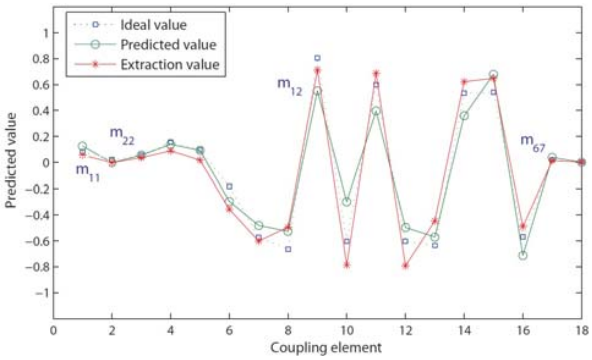

Fig. 8 The prediction value of the coupling matrix

IV. MODELING AND TUNING OF SYSTEM

The main idea of coaxial cavity filter tuning is to accomplish the task by establishing an alternative model of the actual filter. In this way, the tuning problem of the filter is transformed into the parameter optimization problem of the alternative model.

A. Establishment of Tuning System Model

Before the system is modeled, it is necessary to normalize the input and output data according to $x = (x - x_{\min})/(x_{\max} - x_{\min})$, where, $x_{\max}$ is the maximum value of the sample data, $x_{\min}$ is the minimum value of the sample data.

The first layer in Fig. 6 is the input layer. The input layer sample set is $d_i = (d_1, d_2, \cdots, d_8)^{\mathrm{T}}$. The input layer contains m neurons, the second and third layers have i and j neurons respectively, and the output layer has p neurons. ω_{mn} is the weight from the input layer to the hidden layer, ω_{ij} is the weight from the hidden layer to the output layer. ω_{Rij}, ω_{Iij} represent the weights of the real and imaginary parts respectively. The real and imaginary input signals of the hidden layer are:

$$u_{Ri}^{m} = \sum_{1}^{r} \omega_{Rri} \cdot d_{ir} \quad u_{Ii}^{m} = \sum_{1}^{r} \omega_{Iri} \cdot d_{ir}, \tag{20}$$

the real and imaginary output signals of the hidden layer are:

$$u_{Rp}^{p} = f(u_{Rp}^{p}) \quad u_{Ip}^{p} = f(u_{Ip}^{p}), \tag{21}$$

an error signal of p neurons in the output layer:

$$e_{Rp} = m'_{Rp} - m_{Rp} \quad e_{Ip} = m'_{Ip} - m_{Ip}, \tag{22}$$

the total error of output is:

$$E(n) = \frac{1}{2}\sum_{p=1}^{P}\left[\left(m'_{Rp} - m_{Rp}\right)^2 + \left(m'_{Ip} - m_{Ip}\right)^2\right], \tag{23}$$

where $m_{ij} = (m_{11}, m_{12}, \cdots, m_{78})^{\mathrm{T}}$ is the actual output sample set, $m'_{ij} = (m'_{11}, m'_{12}, \cdots, m'_{78})^{\mathrm{T}}$ is expected output. According to the rules of Delta learning, the weights between the output layer and the hidden layer are as follows:

$$\begin{aligned}\Delta\omega_{RjP}(n) &= -\eta\frac{\partial E(n)}{\partial\Delta\omega_{RjP}(n)} = -\eta\frac{\partial E(n)}{\partial\Delta u_{RjP}(n)}\cdot\frac{\partial\Delta u_{RjP}(n)}{\partial\Delta\omega_{RjP}(n)}\\ \Delta\omega_{RjP}(n+1) &= \omega_{RjP}(n) + \Delta\omega_{RjP}(n)\\ \Delta\omega_{IjP}(n+1) &= \omega_{IjP}(n) + \Delta\omega_{IjP}(n).\end{aligned} \tag{24}$$

Similarly, the weights between the hidden layer and the input layer can also be obtained in the same way, in the formula, $\Delta\omega_{RjP}(n)$ represents the weights between the output layer and the hidden layer, $\eta = \left[1/(1+\exp(-ax))\right] + b$, a is the slope parameter of the Sigmoid function, x is the random number within the $[-1,-1]$ interval. The parameter b value depends on the situation. The number of iterations is 20 times, the iteration time is 1s, and the output error is 0.0553. Gradient descent method is used for training. As can be seen from the Error Histogram with 20 Bins in Fig. 7, the curve obeys a normal distribution, which indicate the model is valid.

By establishing the tuning model, we can predict the variation trend of element values in the coupling matrix. The abscissa in the Fig. 8 is the element in the coupling matrix, and the ordinate is the corresponding value of the coupling element. Through the verification of the experiment, the accuracy of the tuning model can meet the requirements of post-tuning.

B. Tuning Based on Field Data

The purpose of tuning is to obtain the best screw position so that the scattering parameters of the filter can meet the performance indicators. In this paper, the mapping relation between the ideal model and the actual model is established by the improved space mapping algorithm, which can guide the tuning amplitude and the tuning direction of the filter. The ideal model parameters are represented by $x_c^j = (m_{11}^j, m_{12}^j, \cdots m_{78}^j)^{\mathrm{T}}$, and the corresponding response is $R_c(x_c)$. The parameters of the actual model are represented as $x_f^j = (d_1^j, d_2^j, \cdots d_8^j)^{\mathrm{T}}$, the corresponding output response is $R_f(x_f)$. By optimizing the parameters $x_c^{(j)}$, let $P(x_f) - x_c^* = 0$. x_c^* is the optimal parameters and $x_f^{(j+1)}$ is obtained by the iteration of $x_f^{(j+1)} = x_f^{(j)} + h^{(j)}$, $h^{(j)}$ is obtained by $(B^{(j)^{\mathrm{T}}}B^{(j)} + \mu I)h^{(j)} = B^{(j)^{\mathrm{T}}}(x_c^* - x_c^{(j)})$, μ is the selection parameter and satisfies $\left\|h^{(j)}\right\| \le \zeta$, ζ is the radius of the confidence range.

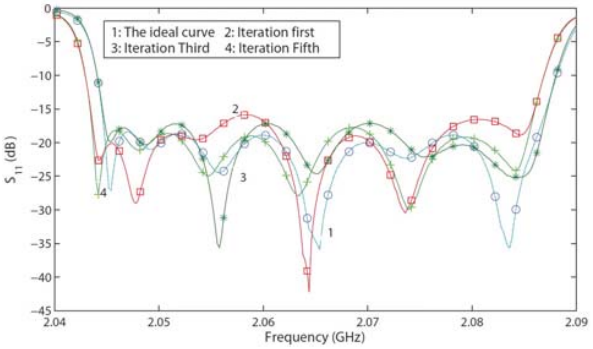

Fig. 9 Comparison of tuning S_{11} and standard S_{11}

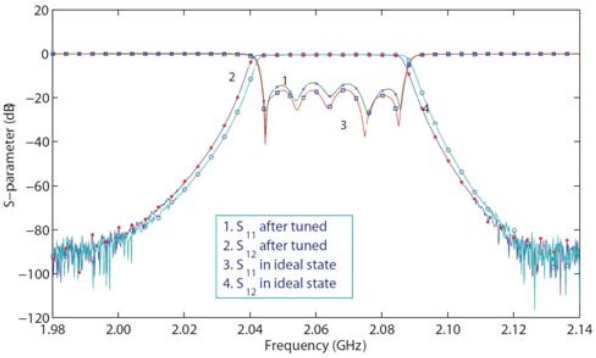

Fig. 10 Changes of S-parameter before and after tuning

The tuning of the coaxial cavity filter can be transformed into the following optimization problem:

$$x_f^* = \arg\min_x U(R(x)) \tag{25}$$

where, x_f^* is the optimal solution of the parameter to be solved, U is the objective function. $B^{(j)}$ is the approximation of the Jacobian matrix, which is updated by following equation:

$$B^{(j+1)} = B^{(j)} + (f^{(j+1)}h^{(j)^{\mathrm{T}}})\Big/(h^{(j)^{\mathrm{T}}}h^{(j)}) \tag{26}$$

It can be seen from the Fig. 9 and the Fig. 10 that after several iterations of the improved space mapping algorithm, the S_{11} and the S_{12} can be matched with the ideal S-parameter after several iterations. By iterative optimization, the return loss can be controlled within -18 dB, the insertion loss is more than -0.8 dB, the passband width is 0.056 GHz, and the maximum value of VSWR is 1.05. The attenuation in 2.037-2.085 GHz is greater than 2 and the attenuation in 2.090-2.096 GHz is greater than 22. The indicators obtained show that the tuned filter can meet the design requirements.

V. Conclusions

In order to obtain the actual variation amount of the actual filter for each screw tuning. This article presents a tuning method based on complex Neural Network and improved Space mapping. The method uses phase error to guide the rotation magnitude and the rotation direction of the screws when the detuning is large. When the detuning of the filter is

small, the coupling matrix is extracted from the S-parameters and the filter tuning model is established. The phase shift and filter loss are processed in the process of parameter extraction. According to the tuning model, the mapping relation between the actual filter and the ideal filter is established. An improved space mapping algorithm is used to update the location of the tuning screws. The experiment of the eight order coaxial cavity filter shows that the system can achieve the desired tuning purpose well.

Acknowledgment

This work was supported by the Hubei Provincial Natural Science Foundation of China under Grant 2015CFA010 and the 111 project under Grant B17040.

References

[1] Y. Min, Robotic Computer-Aided Tuning, *COM DEV internal report*, vol. 6, pp. 11-17, 1994.
[2] Y. Min, Y. Wang, Robotic Computer-Aided Tuning, *IEEE Trans. Microw. J*, vol. 26, pp. 13-16, 2006.
[3] V. Miraftab, R. R. Mansour, Computer-Aided Tuning of Microwave Filters Using Fuzzy Logic, *IEEE Trans. Microwave Theory Tech*, vol. 50, pp. 2781-2788, 2002.
[4] J. Dunsmore, Tuning band pass fliters in the time domain, *IEEE Micro. Symp*. Santa Rosa, 1999, pp. 1351-1354.
[5] R Wang, L. Z Li, L Peng, Diagnosis of Coupled Resonator Bandpass Filters Using VF and Optimization Method, *Progress In Electromagnetics Research M*, vol. 51, 195-203, 2016.
[6] G. Macchiarella, D. Traina, A formulation of the Cauchy method suitable for the synthesis of lossless circuit models of microwave filter from lossy measurements," *IEEE Microw Wireless Compon. Lett*, vol. 16, pp. 243-245, 2006.
[7] C. K. Liao, C. Y. Chang, J. Lin, A Vector-Fitting Formulation for Parameter Extraction of Lossy Microwave Filters, *IEEE Microw Wireless Compon. Lett*, vol. 17, pp. 277-279, 2007.
[8] A. Ghadiya, Parameter Extraction of Direct-Coupled Resonator Filter, *14th Int. Conf. Communication Systems and Network Technologies*, Bhopal, India, 2014, pp. 25-29.
[9] J. Zhou, B. Duan, J. Huang, Support-vector modeling of electromechanical coupling for microwave filter tuning, *IEEE J. RF and Microwave Computer-Aided Engineering*, vol 23, pp. 127-139, 2013.
[10] Y. L. Zhang, J. X. YanA, hybrid computer-aided tuning method for microwave filters with asymmetrical phase shift effects, *Asia-pacific Microw. Conf*. Nanjing, vol. 2, 2015, pp. 6-9.
[11] S. Burger, M. Hoeft, Improved Filter Tuning in the Time Domain Improved Filter Tuning in the Time Domain, *1st Microw. Symp*, Australian, 2015, pp. 27-28.
[12] L. Leifsson, S. Koziel, Surrogate modelling and optimization using shape-preserving response prediction: A review, *Engineering Optimization*, vol. 48, pp. 476-496, 2016.
[13] J. J. Michalski, Artificial neural network algorithm for automated filter tuning with improved efficiency by usage of many golden filters, *18th Int. Conf. MIKON*, Vilnius, Lithuania, 2010 pp. 14-16.
[14] Q. S. Cheng, J. W. Bandler, S. Koziel, A review of implicit space mapping optimization and modeling techniques, *IEEE MTT-S Int. Conf. NEMO*, Ottawa, Aug, 2015, pp. 11-14.
[15] G. Macchiarella, "Extraction of unloaded Q and coupling matrix from measurements on filters with Large losses," *IEEE Microw Wireless Compon. Lett*, vol. 6, pp. 307-309, Jun. 2010.
[16] P. Kozakowski, Automated CAD of Coupled Resonator Filters, *IEEE Trans. Microwave Theory Tech*, vol. 12, December, pp. 470-472, 2002.
[17] H. Hu, K. L. Wu, A Generalized Coupling Matrix Extraction Technique for Bandpass Filters With Uneven-Qs, *IEEE Trans. Microwave Theory Tech,* vol. 62, pp. 244-251, 2014.
[18] R. I. Cameron, Advanced coupling matrix synthesis techniques for microwave filters, *IEEE Trans. Microwave Theory Tech*, vol. 51, pp. 1-10, Jan. 2003.